Electronic Supplementary Information (ESI) for Journal of CrystEngComm.

This journal is © The Royal Society of Chemistry 2018

***SUPPORTING INFORMATION***

# Fluorogenic Naked-Eye Sensing and Live-Cell Imaging of Cyanide by Hydrazine-Functionalized CAU-10 Metal-Organic Framework

*Rana Dalapati,[a] Soutick Nandi,[a] Helge Reinsch,[b] Bibhas K. Bhunia,[c] Biman B. Mandal,[c] Norbert Stock,[b] and Shyam Biswas *,[a]*

[a] Department of Chemistry, Indian Institute of Technology Guwahati, Guwahati, 781039 Assam, India.

[b] Institut für Anorganische Chemie, Christian-Albrechts-Universität, Max-Eyth-Strasse 2, 24118 Kiel, Germany.

[c] Biomaterial and Tissue Engineering Laboratory, Department of Biosciences and Bioengineering, Indian Institute of Technology, Guwahati, Guwahati, Assam 781035, India

* To whom correspondence should be addressed.
E-mail: sbiswas@iitg.ernet.in. Tel: (+)91-3612583309. Fax: (+)91-3612582349.

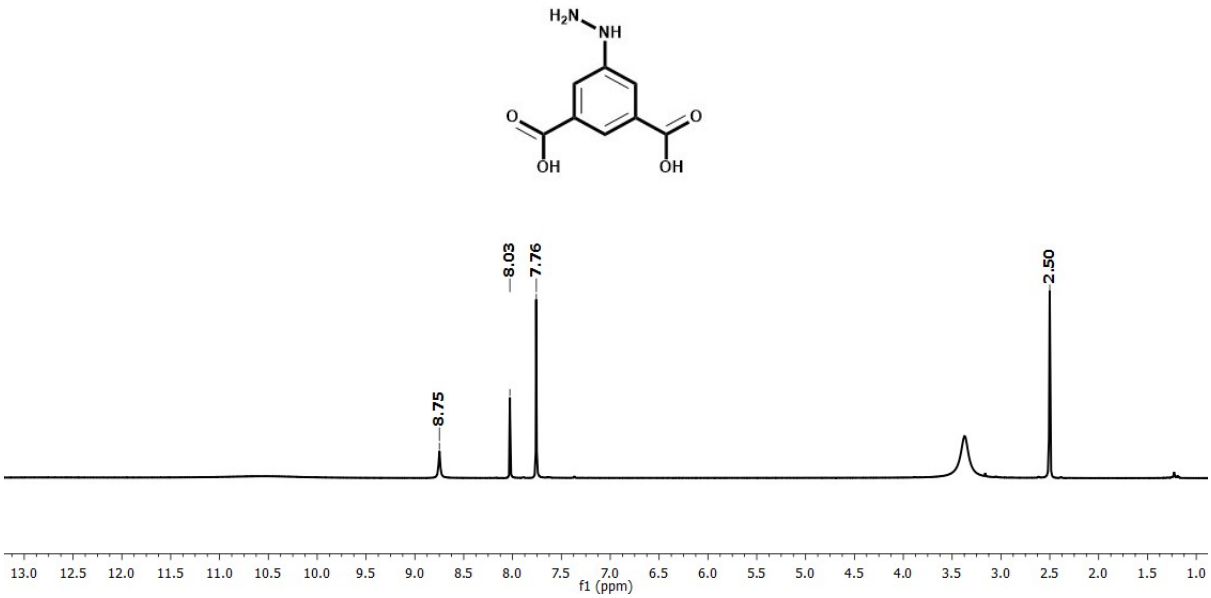


**Figure S1.** $^{1}$H NMR spectrum of $H_2$IPA-$N_2H_3$ ligand measured in DMSO-$d_6$.

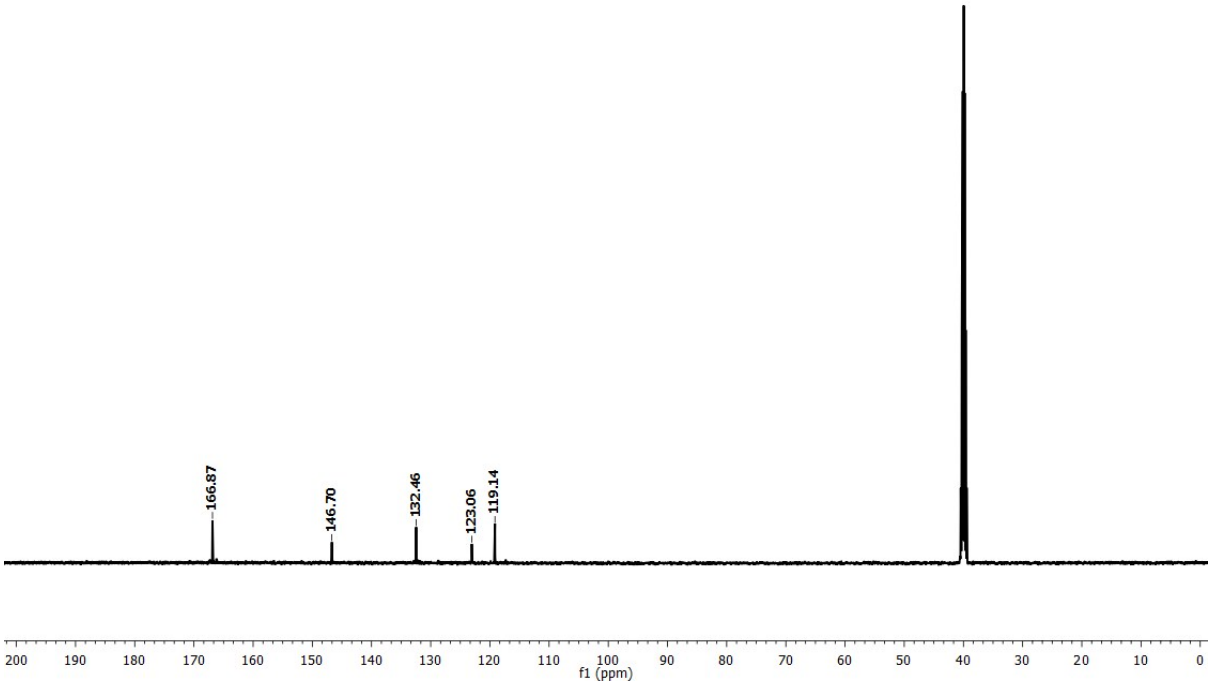


**Figure S2.** $^{13}$C NMR spectrum of $H_2$IPA-$N_2H_3$ ligand measured in DMSO-$d_6$.

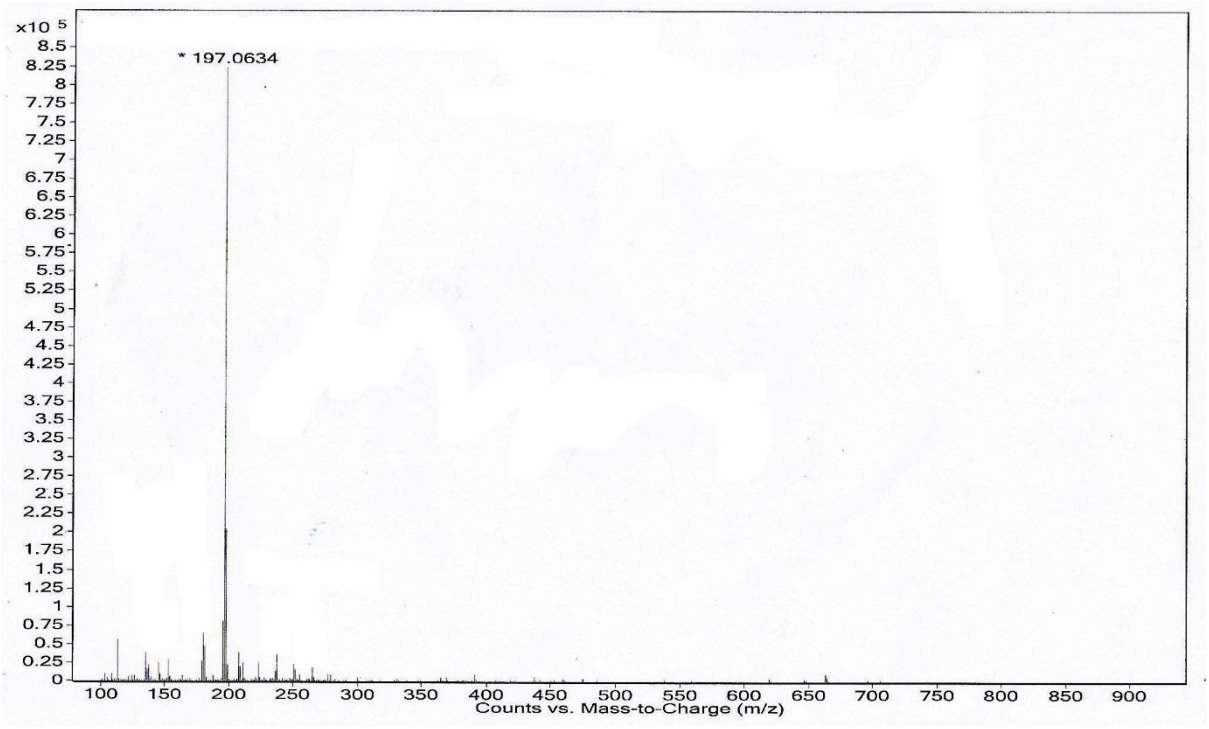


**Figure S3.** ESI-MS spectrum of $H_2$IPA-$N_2H_3$ ligand.

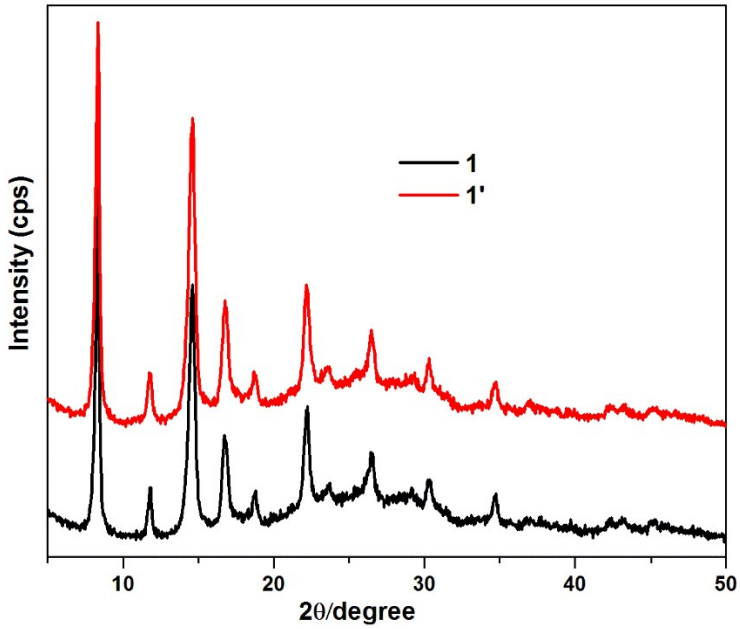


**Figure S4.** XRPD patterns of as-synthesized **1** and thermally activated **1'**.

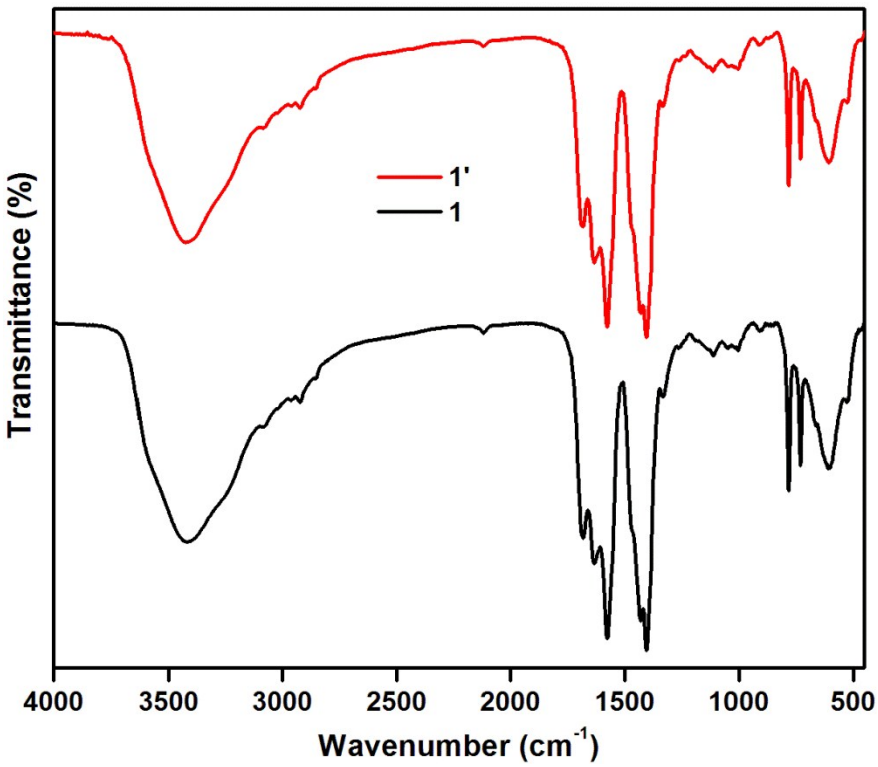


**Figure S5.** FT-IR spectra of as-synthesized **1** and thermally activated **1'**.

**Table S1.** Pawley refinement parameters for **1** and **1'**.

| Compound | **1** | **1'** |
|---|---|---|
| space group | $I4_1/a$ | $I4_1/a$ |
| $a = b$ [Å] | 21.379(16) | 21.395(12) |
| $c$ [Å] | 11.346(8) | 11.223(6) |
| $\alpha = \beta = \gamma$ [°] | 90 | 90 |
| $R_{WP}$ [%] | 3.3 | 3.6 |
| GoF | 2.2 | 2.4 |

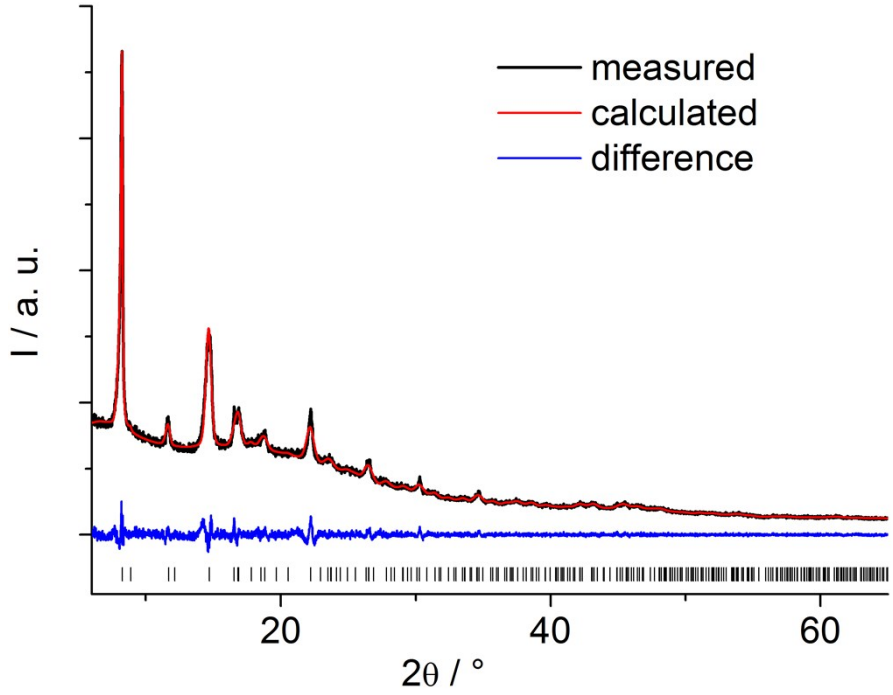


**Figure S6.** Final Pawley refinement plot for activated **1**. The black curve represents the measured data and the red curve is the theoretical data. The vertical black bars mark the allowed Bragg reflection positions.

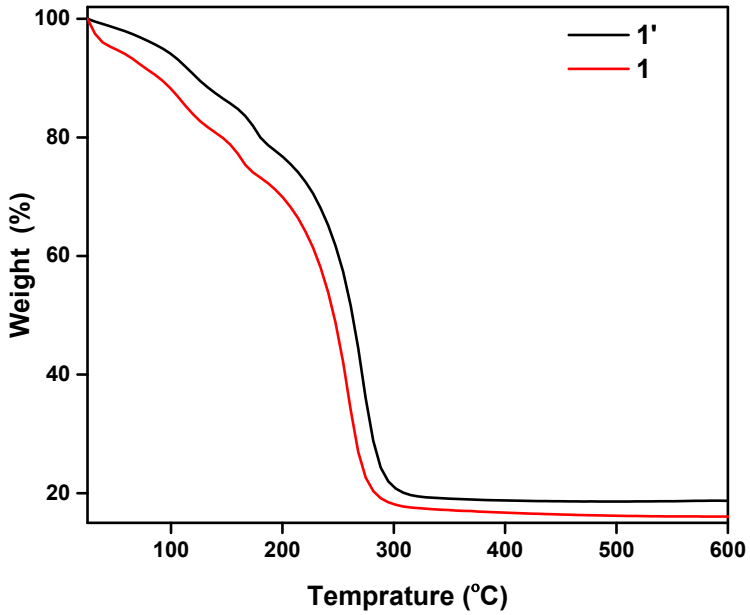


**Figure S7.** TG curves of **1** and **1'** recorded in an air atmosphere in the temperature range of 25-600 °C with a heating rate of 5 °C $min^{-1}$.

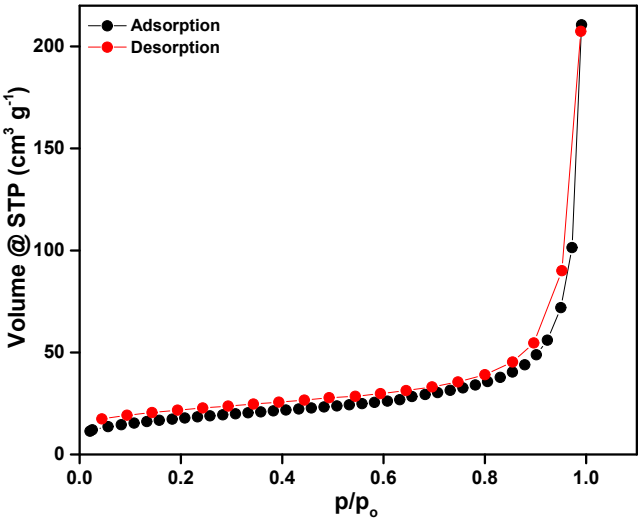


**Figure S8.** $N_2$ adsorption (black circles) and desorption (red circles) isotherms of **1'** recorded at –196 °C.

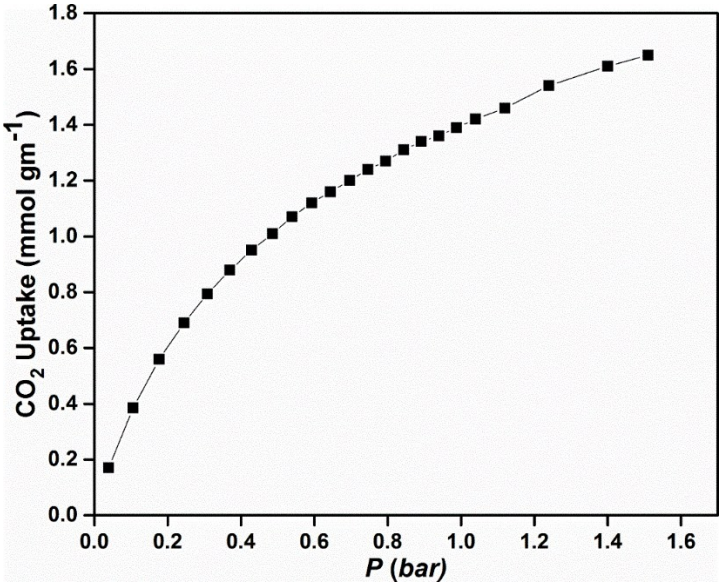


**Figure S9.** $CO_2$ adsorption of **1'** recorded at 25 °C.

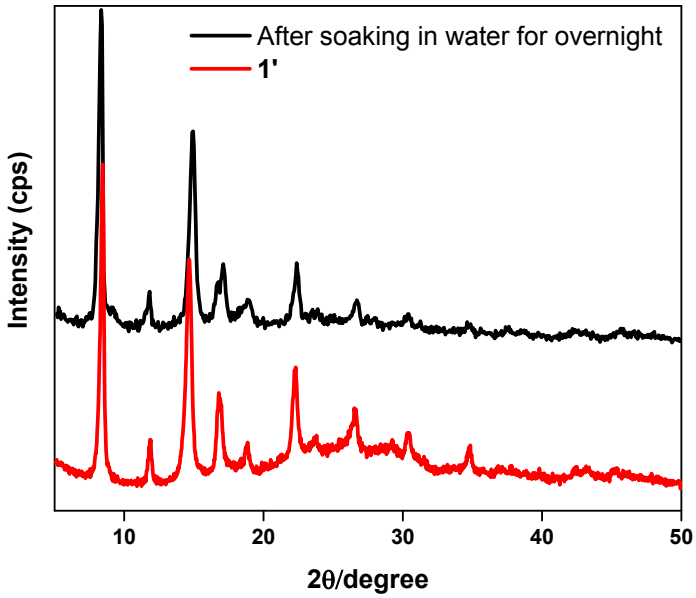


**Figure S10.** XRPD pattern of **1'** after soaking in water for overnight.

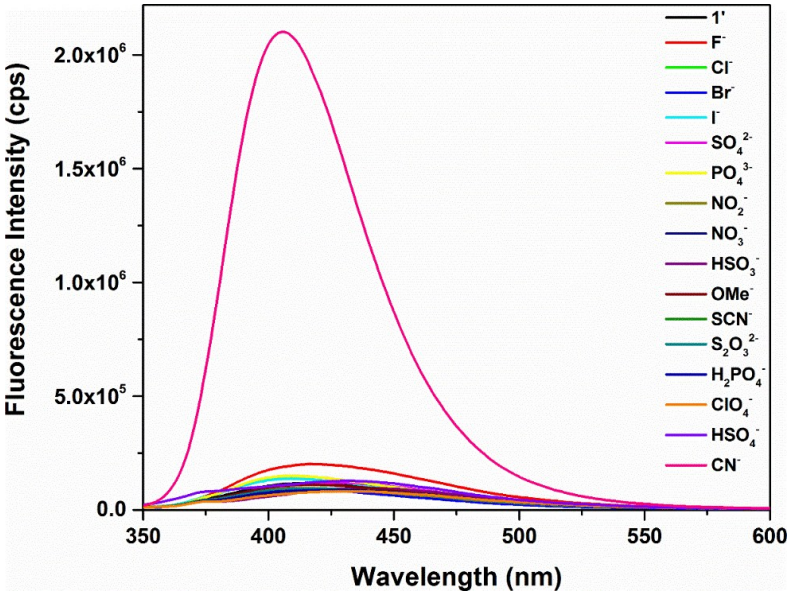


**Figure S11.** Change in the fluorescence intensity of **1'** upon addition of 4 mM solution (500 μL) of various anions.

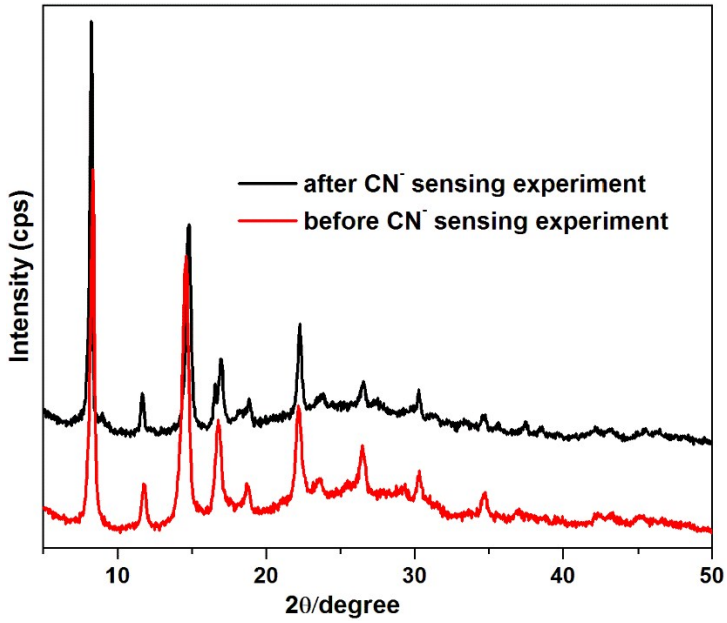


**Figure S12.** XRPD patterns of **1'** before and after the $CN^-$ sensing experiment.

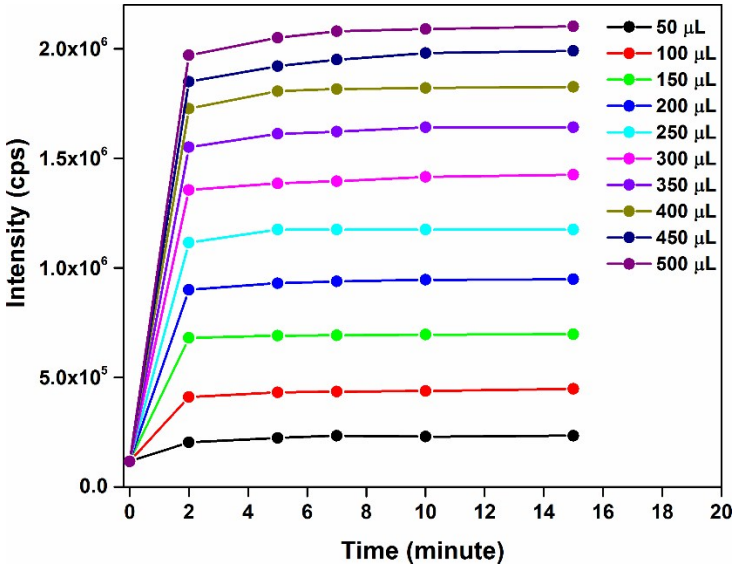


**Figure S13.** Time-dependent change in the fluorescence intensity of **1'** upon addition of different concentrations of $CN^-$ ion.

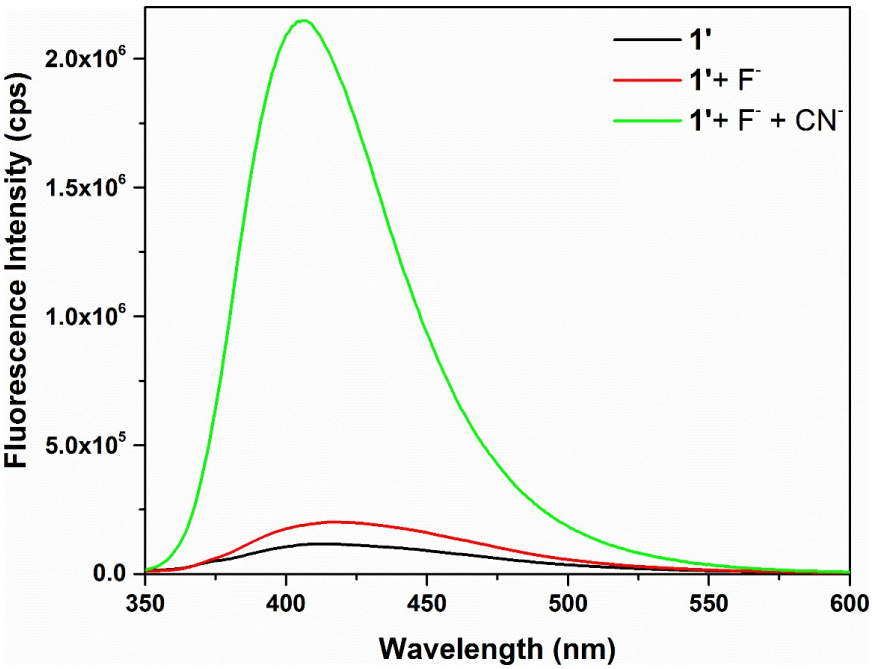


**Figure S14.** Change in the fluorescence intensity of **1'** upon addition of 4 mM $CN^-$ solution (500 µL) in presence of $F^-$ ion (500 µL).

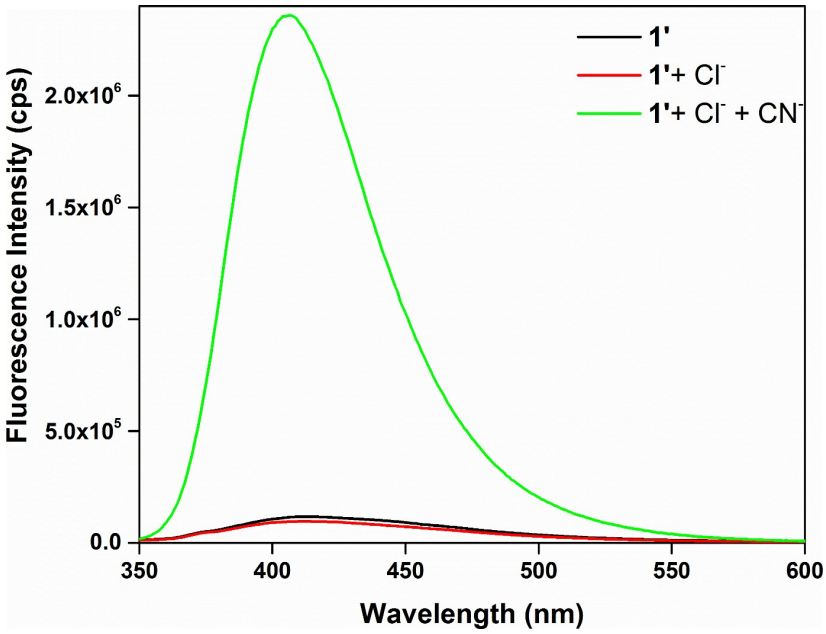


**Figure S15.** Change in the fluorescence intensity of **1'** upon addition of 4 mM $CN^-$ solution (500 µL) in presence of $Cl^-$ ion (500 µL).

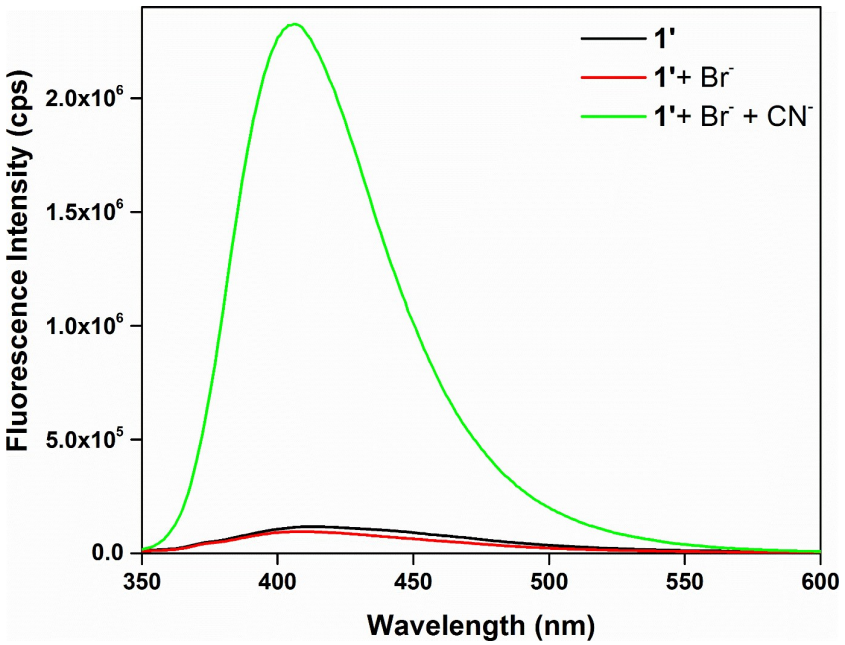


**Figure S16.** Change in the fluorescence intensity of **1'** upon addition of 4 mM $CN^-$ solution (500 µL) in presence of $Br^-$ ion (500 µL).

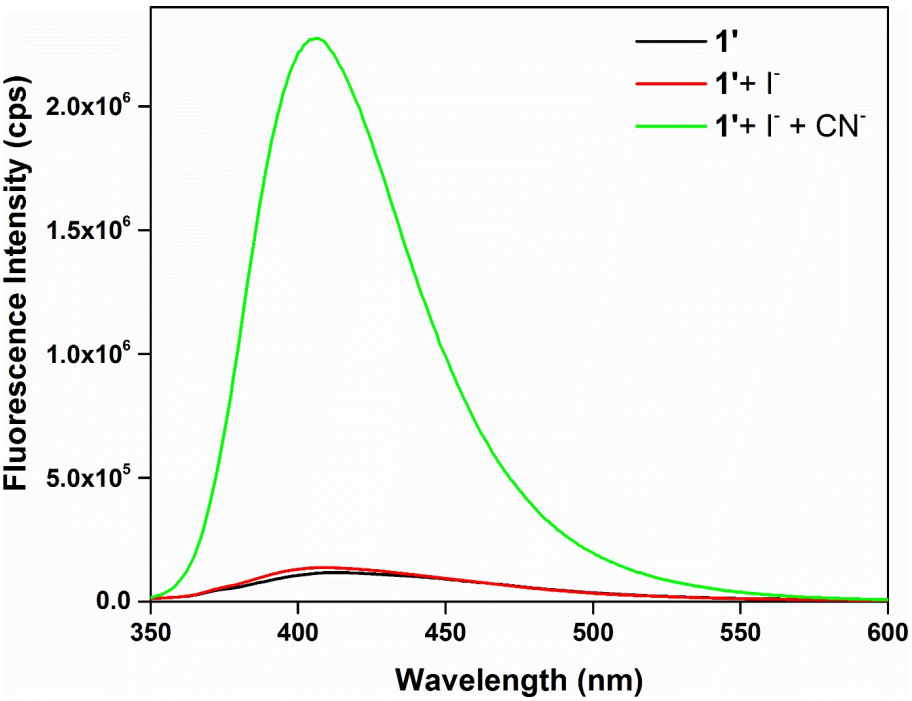


**Figure S17.** Change in the fluorescence intensity of **1'** upon addition of 4 mM $CN^-$ solution (500 µL) in presence of $I^-$ ion (500 µL).

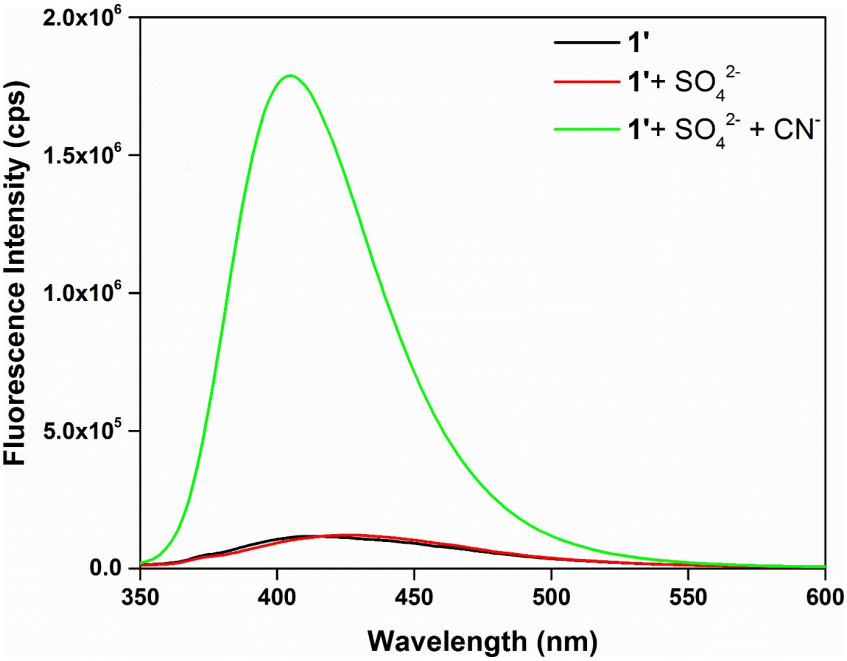


**Figure S18.** Change in the fluorescence intensity of **1'** upon addition of 4 mM $CN^-$ solution (500 µL) in presence of $SO_4^{2-}$ ion (500 µL).

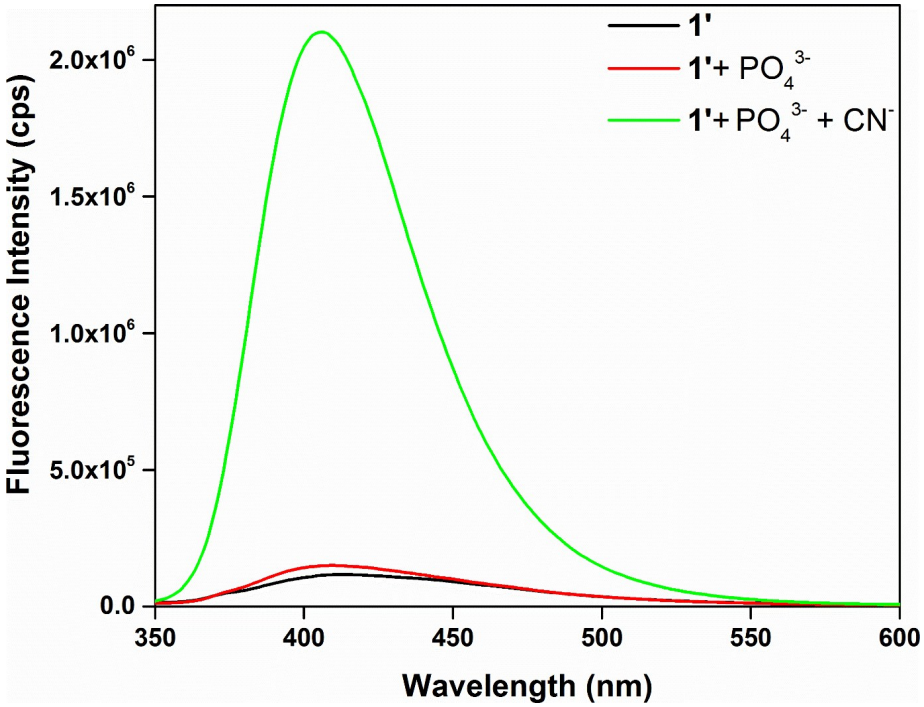


**Figure S19.** Change in the fluorescence intensity of **1'** upon addition of 4 mM $CN^-$ solution (500 µL) in presence of $PO_4^{3-}$ ion (500 µL).

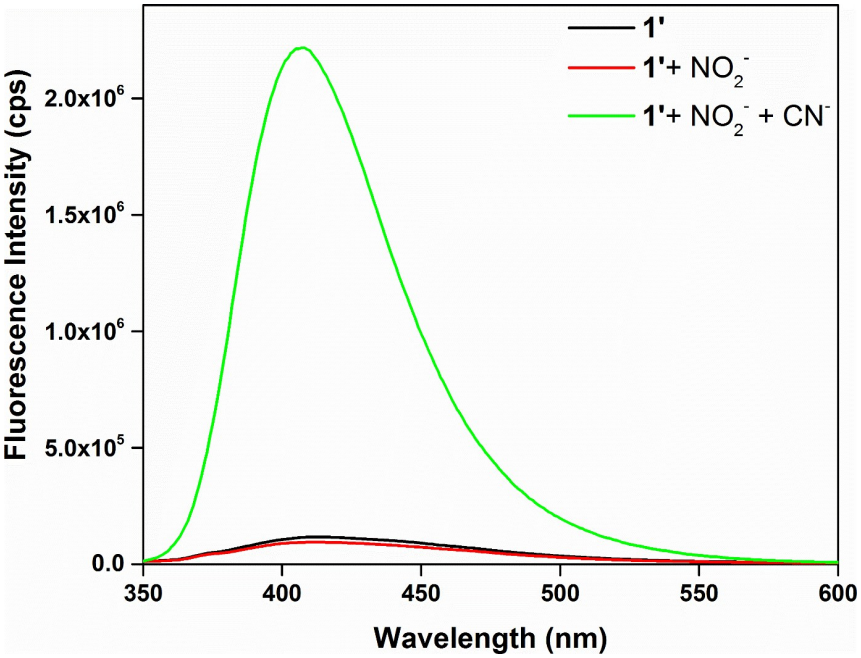


**Figure S20.** Change in the fluorescence intensity of **1'** upon addition of 4 mM $CN^-$ solution (500 µL) in presence of $NO_2^-$ ion (500 µL).

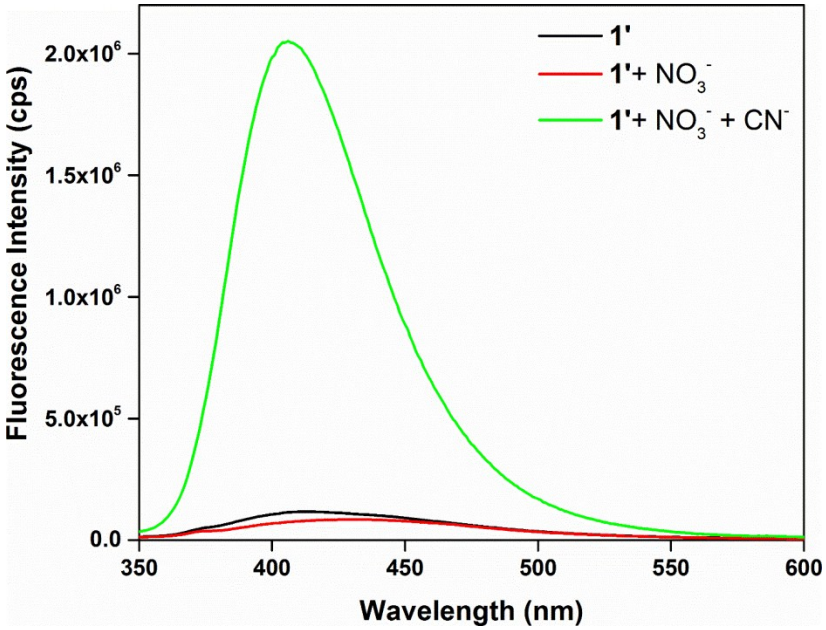


**Figure S21.** Change in the fluorescence intensity of **1'** upon addition of 4 mM $CN^-$ solution (500 µL) in presence of $NO_3^-$ ion (500 µL).

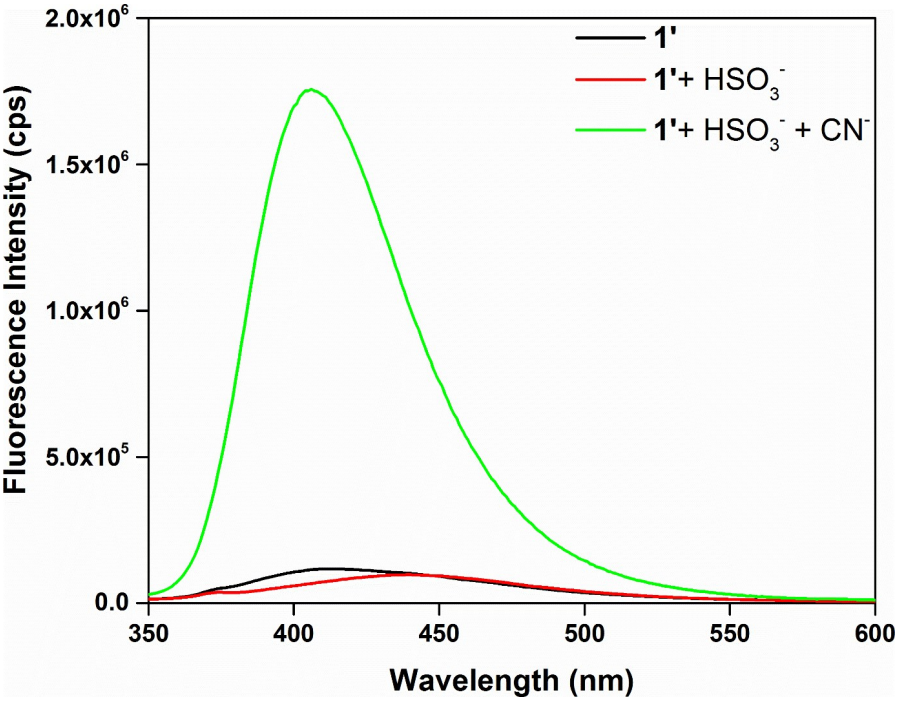


**Figure S22.** Change in the fluorescence intensity of **1'** upon addition of 4 mM $CN^-$ solution (500 µL) in presence of $HSO_3^-$ ion (500 µL).

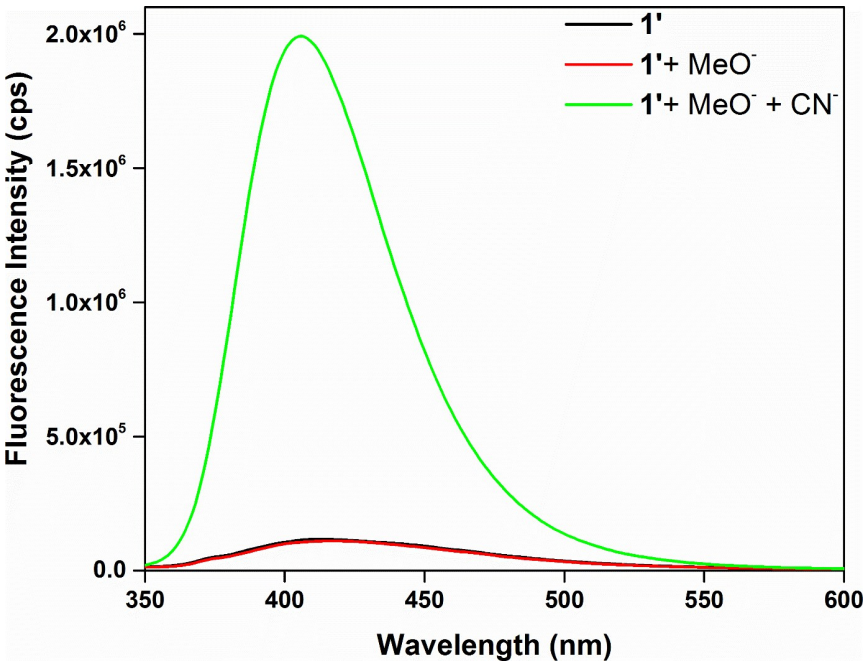


**Figure S23.** Change in the fluorescence intensity of **1'** upon addition of 4 mM $CN^-$ solution (500 µL) in presence of $HSO_3^-$ ion (500 µL).

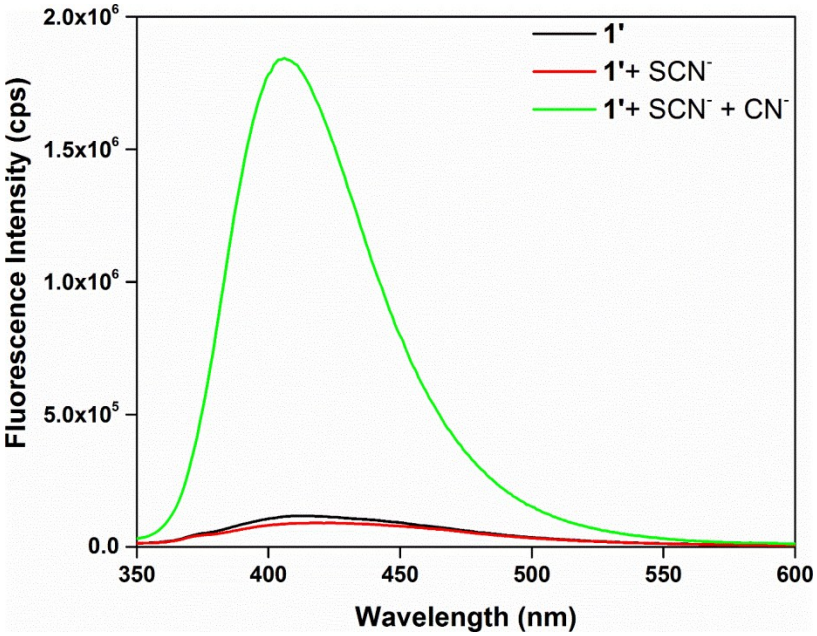


**Figure S24.** Change in the fluorescence intensity of **1'** upon addition of 4 mM $CN^-$ solution (500 µL) in presence of $SCN^-$ ion (500 µL).

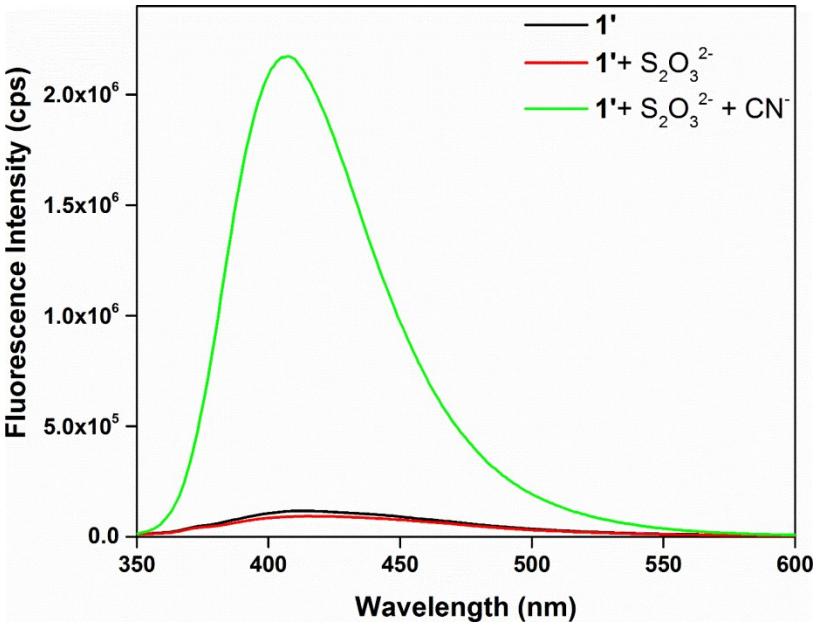


**Figure S25.** Change in the fluorescence intensity of **1'** upon addition of 4 mM $CN^-$ solution (500 µL) in presence of $S_2O_3^{2-}$ ion (500 µL).

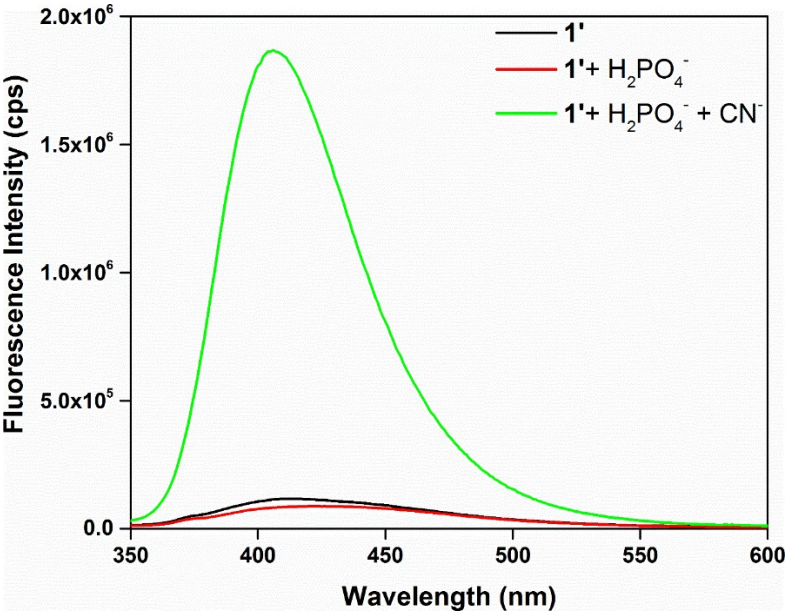


**Figure S26.** Change in the fluorescence intensity of **1'** upon addition of 4 mM $CN^-$ solution (500 µL) in presence of $H_2PO_4^-$ ion (500 µL).

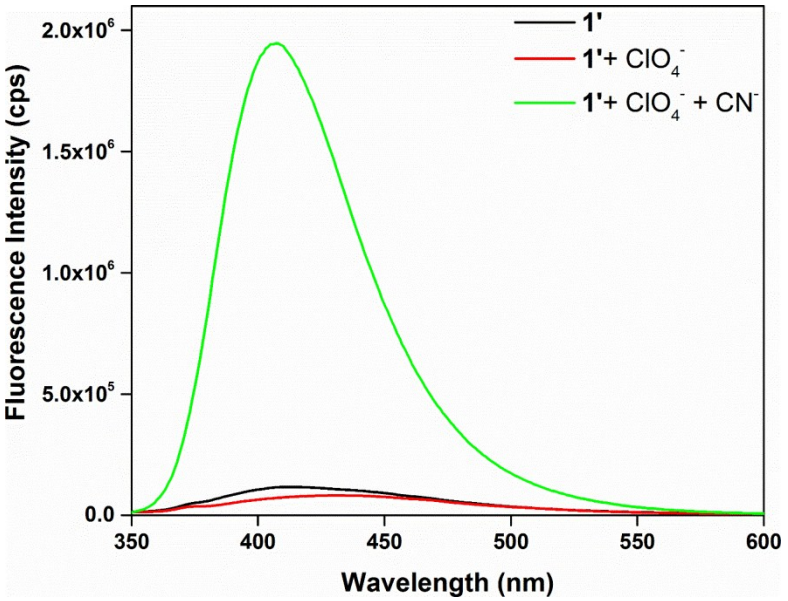


**Figure S27.** Change in the fluorescence intensity of **1'** upon addition of 4 mM $CN^-$ solution (500 µL) in presence of $ClO_4^-$ ion (500 µL).

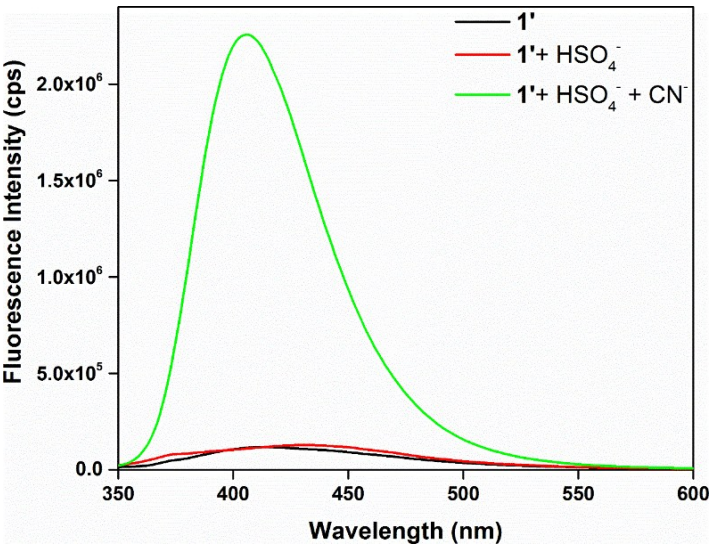


**Figure S28.** Change in the fluorescence intensity of **1'** upon addition of 4 mM $CN^-$ solution (500 µL) in presence of $HSO_4^-$ ion (500 µL).

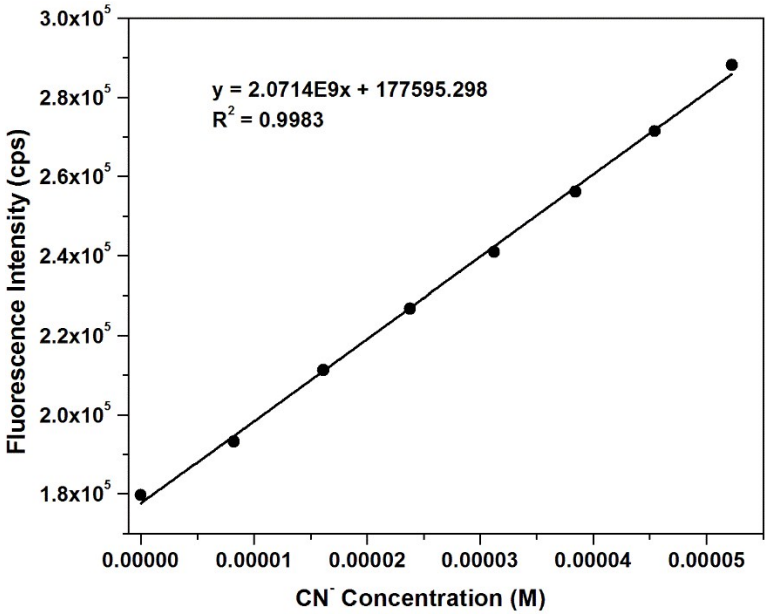


**Figure S29.** Change in the fluorescence intensity of **1'** in aqueous solution as a function of $CN^-$ concentration.

**Table S2.** Comparison of the various existing fluorescent materials for the sensing of $CN^-$.

| Sl. No. | Sensor Material | Type of Material | Sensing Medium | Detection Limit | Ref. |
|---|---|---|---|---|---|
| 1 | CAU-10-$N_2H_3$ | MOF | Water | 0.48 μM | This work |
| 2 | M-ZIF-90 | MOF | DMSO/$H_2O$ | 2 μM | 1 |
| 3 | Carbazole-functionalized Zr(IV) MOF | MOF | Water | 0.14 μM | 2 |
| 4 | Bio-MOF-1⊃DAAC | MOF | HEPES buffer | 5.2 ppb | 3 |
| 5 | Tb-ADP-Bipy MOF | MOF | Water | 30 nM | 4 |
| 6 | PAT–TFBE | Gel | Water | 1.82 μM | 5 |
| 7 | BP | benzopyrylium–phenothiazine conjugate | $CH_3CN/H_2O$ | 0.13 μM | 6 |
| 8 | NBD-SSH−$Cu^{2+}$ | peptide-based ensemble | Water | 24.9 nM | 7 |
| 9 | Pyridyl azo-based chemosensors | Gel | Sol-gel medium | 9.36 μM | 8 |
| 10 | pyridinium-fused pyridinone iodide | Chemodosimeter | THF/ $H_2O$ | 54 nM | 9 |
| 11 | 3 T-2CN | Oligothiophene chemosensor | DMSO/$H_2O$ | 0.19 μM | 10 |
| 12 | AuAgNCs@ew | bimetallic gold−silver nanoclusters | Water | 0.138 μM | 11 |
| 13 | $\{Ru^{II}(^tBubpy)(CN)_4-[Cu^{II}(dien)]_3\}(ClO_4)_2$ | trinuclear heterobimetallic Ru(II)−Cu(II) complex, | DMF/$H_2O$ | 1.2 μM | 12 |
| 14 | receptor 1 | DMN conjugated benzothiazole | DMF/$H_2O$ | 0.16 μM | 13 |
| 15 | PNA⊃GBP·$I_2$ | supramolecular polymer | DMSO–$H_2O$ | 41 nM | 14 |

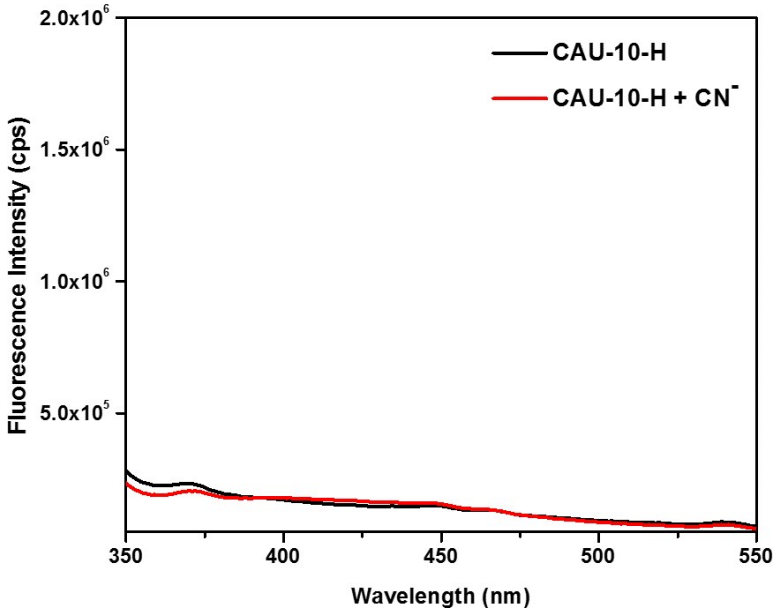


**Figure S30.** Change in the fluorescence intensity of CAU-10-H upon addition of 4 mM solution (500 µL) of aqueous $CN^-$ solution.

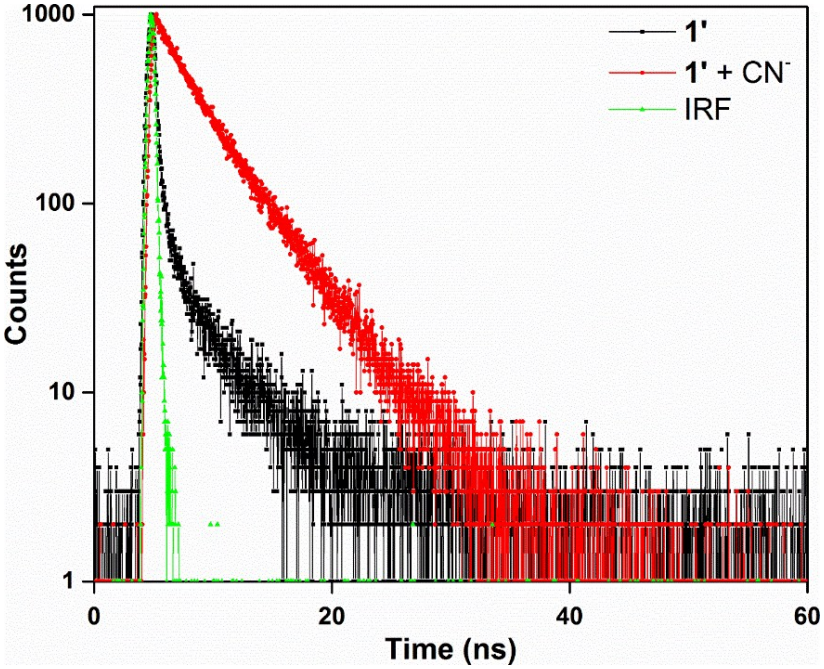


**Figure S31.** Lifetime decay profile of **1'** in presence of aqueous $CN^-$ solution ($\lambda_{ex}$ = 336 nm, monitored at 430 nm).

**Table S3.** Average excited-state lifetime (<τ>) values of **1'** before and after addition of $CN^-$ solution ($\lambda_{ex}$ = 336 nm).

| Volume of $CN^-$ solution added (μL) | $a_1$ | $a_2$ | $\tau_1$ (ns) | $\tau_2$ (ns) | <τ>* (ns) | $\chi^2$ |
|---|---|---|---|---|---|---|
| 0 | 0.981 | 0.019 | 0.310 | 3.866 | 0.377 | 1.09 |
| 500 | 0.153 | 0.846 | 0.778 | 4.784 | 4.161 | 1.01 |

* $\langle\tau\rangle = a_1\tau_1 + a_2\tau_2$

## References


1. A. Karmakar, N. Kumar, P. Samanta, A. V. Desai and S. K. Ghosh, *Chem. - Eur. J.*, 2016, **22**, 864-868.
2. A. Das and S. Biswas, *Sens. Actuators, B*, 2017, **250**, 121-131.
3. A. Karmakar, B. Joarder, A. Mallick, P. Samanta, A. V. Desai, S. Basu and S. K. Ghosh, *Chem. Commun.*, 2017, **53**, 1253-1256.
4. L. Wang, S. Wang and Y. Chen, *Microchim. Acta*, 2017, **184**, 4597-4602.
5. H. Fang, G. Cai, Y. Hu and J. Zhang, *Chem. Commun.*, 2018, **54**, 3045-3048.
6. S. Mondal, S. S. Ali, S. Manna, K. Maiti, M. R. Uddin, S. Mandal, D. Mandal and A. K. Mahapatra, *New J. Chem.*, 2017, **41**, 12581-12588.
7. K. H. Jung and K.-H. Lee, *Anal. Chem.*, 2015, **87**, 9308-9314.
8. A. Panja and K. Ghosh, *ChemistrySelect*, 2018, **3**, 1809-1814.
9. J. Li, J. Gao, W. W. Xiong, P. Z. Li, H. Zhang, Y. Zhao and Q. Zhang, *Chem. - Asian J.*, 2014, **9**, 121-125.
10. L. Lan, T. Li, T. Wei, H. Pang, T. Sun, E. Wang, H. Liu and Q. Niu, *Spectrochim. Acta, Part A*, 2018, **193**, 289-296.
11. L. Tian, Y. Li, T. Ren, Y. Tong, B. Yang and Y. Li, *Talanta*, 2017, **170**, 530-539.
12. C.-F. Chow, M. H. Lam and W.-Y. Wong, *Inorg. Chem.*, 2004, **43**, 8387-8393.
13. K. Keshav, P. Torawane, M. K. Kumawat, K. Tayade, S. K. Sahoo, R. Srivastava and A. Kuwar, *Biosens. Bioelectron.*, 2017, **92**, 95-100.
14. Q. Lin, K.-P. Zhong, J.-H. Zhu, L. Ding, J.-X. Su, H. Yao, T.-B. Wei and Y.-M. Zhang, *Macromolecules*, 2017, **50**, 7863-7871.